Hydrodynamic analysis of a slalom fin of windsurf board

Ana Marta Rodrigues dos Santos
martarsantos@tecnico.ulisboa.pt

Instituto Superior Técnico, Lisboa, Portugal

ABSTRACT: The objective of the thesis is to perform a hydrodynamic analysis in estimating the water-induced loads on a real slalom fin of a windsurf board. First, an initial 2-D flow study of the fin hydrofoil, using the software XFOIL will be performed. This will serve as mean of calibration for the commercial Computational Fluid Dynamics software Star-CCM+. Since the analysed flow is in the range of 3x105 to 10x105 of the Reynolds' number, inside the transition interval, laminar, transition and turbulence models will be used. The 2-D flow study of the hydrofoil and the 3-D flow study of the fin will be conducted using Star-CCM+, to analyse the fluid-structure interaction. This MSc thesis will rely on several research collaborations originating from different Universities from Portugal and the United Kingdom, which may lead to an opportunity of a further cavitation phenomenon investigation.

KEYWORDS: CFD, Star CCM+, Windsurf, Fin, RANS, Aerofoil, $\gamma - Re\theta$ transition model, $k - \omega$ SST

1 INTRODUCTION

Since the early ages, man has designed and crafted vessels that would help on the task of crossing seas, rivers and oceans. Nowadays, man no longer needs to build for the sole purpose of survival: he can use his crafts for leisure as well. At the marine environment, there are several sports and amusements which require the art and know-how skills of artisans, be it windsurf surfboards or small sailing crafts. With modern technology, it is within reach an in-depth engineering study of these crafted arts. Together in symbiosis, art and engineering may lead to improved performance, taking man faster and further into the future.

This work aspires to open a door in the study of crafted windsurf board fins, where an already existing design will be studied and dissected. With the tools available in our century, the flow and fluid-structure interaction can be simulated with accuracy, to pinpoint the aspects of the part that can be improved. Specifically, these tools would be Computational Fluid Dynamics' (CFD), software, a virtual environment where the fin can be pushed to the limits endlessly and at lower costs than those of a towing tank.

A hydrodynamic analysis to a slalom fin for a windsurf board (SFWB) is to be performed. The fin, object of the study, is made by *F-Hot* company, by the designer Steve Cook. The primary objective to develop in this project concerns, but is not exclusive to, the verification of the pressure distribution at the slalom windsurf board fin (SFWB), to be used on another project.

The creation of a foil for marine sports' applications covers many steps, like the structural engineering, the hydrodynamics, durability, fatigue, etc. Despite the comprehensive checklist, the study will focus on the analysis of the flow around the SFWB. It is intended to understand how the flow will develop inside a velocity envelope, and what will be the hydrodynamic loads on the structure. As such, the fin will first be studied in 2-D, where validation of results can be easily assessed. After, the study will be carried out in 3-D. The obtained results will be necessary for other teams to get a feel of the loads employed by the fluid.

2 FIN DESIGN AND PHYSICAL PROPERTIES

A hydrodynamic analysis will be conducted using computational fluid dynamics. The case studies for the analysis comprehend the pre-analysis in 2-D, for a control aerofoil (E387 [2]) and the fin profile. A panel method with viscid formulation software will be used for this objective (XFOIL [3]). This will depict a general idea of the range of values, for pressure,

lift, drag and other phenomena, to be expected per 3-D analysis.

Then, program data obtained for the control aerofoil will be compared to wind-tunnel results to verify the legitimacy of the subsequent fin section 2-D analysis results.

After, using Star-CCM+ [4], a 2-D analysis of the control profile E387 will be performed to verify the physics models to employ, comparing to wind-tunnel and XFOIL data, followed by an identical 2-D flow simulation of the fin profile.

To finish the research, the 3-D analysis of the complete fin will be run on Star-CCM+, using the previously acknowledged simulation parameters.

2.1 *37 RS-3 Standard Slalom Fin*

The object in the study is a slalom fin for windsurfing practice, as in figure 1. The total length, excluding the board attachment box, is of 360.17 mm. The length at root is 100 mm, the rake angle 2°.

The leading edge of the piece is to be the round front, and the trailing edge the straight opposite side.

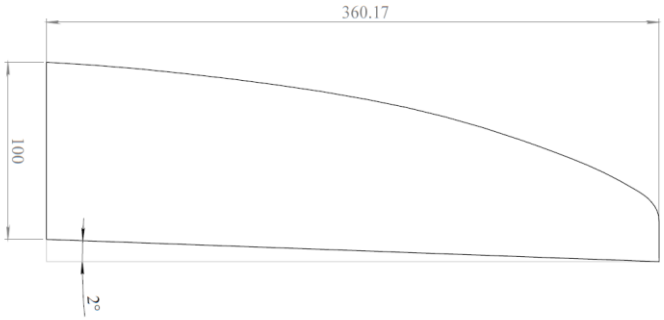

Figure 1: Slalom Windsurf board fin dimensions (all dimensions in mm and degrees)

Considering the root of the fin, three profiles where selected, spaced 100 mm in between and starting 100 mm away from the root, like shown (figure 2):

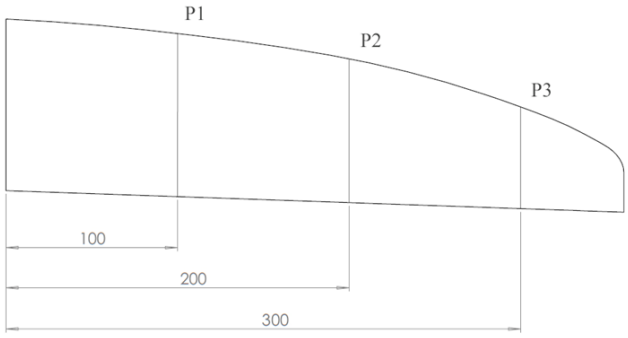

Figure 2: location of the three profiles to be studied, named P1, P2 and P3

The methodology consisted in applying planes normal to the longitudinal direction, developing from leading to trailing edge. This way, the profile and the plane would intersect, producing a line like an aerofoil. The coordinates composing the aerofoils have an increment of 2 mm along the chord, except at the leading edge, which required refinement, thus, more coordinates. The coordinates that define the three profiles were then extracted. After verifying that the planes produce the same aerofoil, the fin was considered of the constant profile. For the 2-D simulations, profile P1 is considered (see figure 3), having a thickness of 8.2 %c at 41.2 %c. It is a symmetric foil. A slight geometry adjustment had to be carried out to mitigate the effect of the foil discretisation.

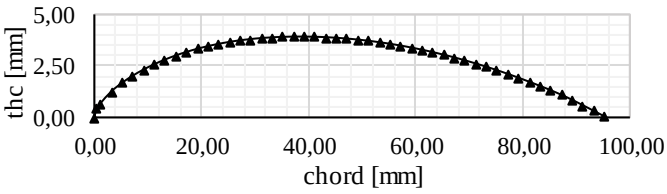

Figure 3: Aerofoil P1 at plane 1, 100 mm from root

2.2 *Physical properties*

To perform the study on the SFWB, it is necessary to know the fluid characteristics. The table 2.1 summarises all the needed seawater parameters with a salinity of 35 g/kg [5] [6], sailing parameters [7] and estimations made.

Table 1: Trial running parameters

Name	Value	Units
Temperature	20	ºC
Density of seawater σ (sea water @ 20 ºC)	1024.9	kg/m3
Kinematic Viscosity υ (sea water @ 20 ºC)	1.050 x10-6	m2s-1
Dynamic Viscosity μ (sea water @ 20 ºC)	1.077 x103	Kg/m.s
Minimum velocity	7.700 (15)	m/s (kn)
Average velocity	10.300 (20)	m/s (kn)
Maximum velocity	25 (50)	m/s (kn)
Minimum Reynolds Number	0.200 x106	
Maximum Reynolds Number	0.750 x106	
Minimum angle of attack	0	°
Maximum angle of attack	15	°

The Reynolds number is based on the minimum and maximum length of the SFWB chord, being highly sensitive to this value.

3 2-D PRE-ANALYSIS

Before the 3-D flow analysis, a two-dimensional study of the characteristics of the SFWB was carried out. There are two main reasons why this course of action was taken.

First, it would help understand in which regime (or regimes), the flow was developing. For example, if the flow at the fin is continuously laminar inside the Reynolds interval, then the computation setting may be simplified, as it makes no sense to apply additional models for transition or turbulence, as it will be discussed ahead. Secondly, by running a known profile with results from the wind tunnel, verify that the

program is being well used and the results obtained from it can be trusted.

XFOIL was the software selected to perform the first analysis. It is seen as a reference in data collection in many certified websites and works, being accessible and intuitive to work with.

3.1 *E387 Analysis*

The Eppler 387 foil was chosen to be the reference for simulations. The data from wind-tunnel experiments is available inside the working intervals of the fin, which is Re of 0.46 x10^6. This is an asymmetric profile that is known to create a recirculation bubble inside the test intervals of Re and AoA.

Comparing the behaviour of the foil between XFOIL and the experimental data displays similar results until 10°. For higher AoA, the results diverge, like in figure 4. Convergence of the results proves difficult from 4° to 6° of AoA.

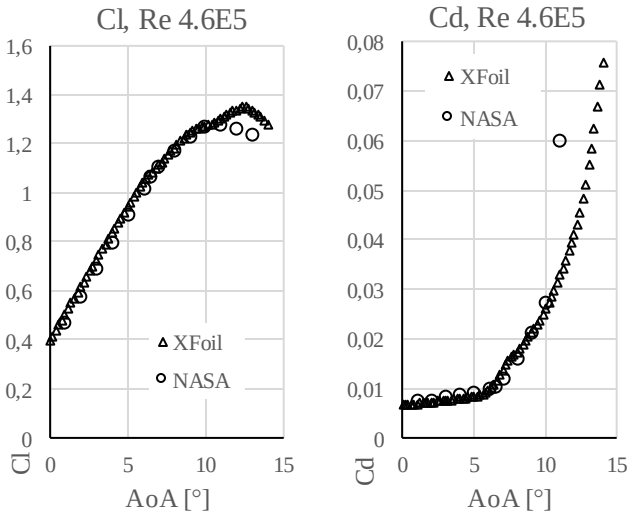

Figure 4: Plots for the C_l and C_d coefficients on E387, using Nasa wind tunnel results and XFOIL results

3.2 *SFWB foil*

These results comprehend the data observed on XFOIL software, for the Reynolds numbers between 0.20 x10^6 to 0.70 x10^6. The angle of attack ranges from 0° to 15°. An example is provided on figure 5 and depicts the results obtained with Re 4.5 x10^5.

The pressure coefficient distribution, plotted to represent the non-dimensional pressure on the surface, showed as expected a maximum value at the nose of the profile at zero degrees. As the angle increases, different values of pressure coefficient are plotted for the upper surface and lower foil surface. As commonly known, at positive AoA and symmetric aerofoils, the pressure is negative on the upper surface and positive on the lower surface. This effect is broadly used to achieve lift on aeroplanes, as the wings are oriented initially on positive AoA's. There is also a *step* in the C_p distribution, close to the tip of the aerofoil, on the upper side. This shows that something unexpected provoked a more severe increase in pressure, like a geometry change, and hints for the generation of a recirculation bubble.

The lift coefficient presents a value of zero at AoA 0°. It showed a linear behaviour generally until 6°; after that, it stalls. Around 9°, the aerofoil seems to regain lift, increasing exponentially. For the first segment, on the linear behaviour, the Cl reaches around 0.65; on the second half of the lift coefficient distribution, the value may go until 0.72.

Regarding the drag coefficient curve, it is starting close to zero at AoA 0°. This is where the drag is minimum, as the profile is in line with the flow. It is seen to increase as the angle of attack increases, to be expected as the exposed area grows, in the way of the flow lines. The minimum observed value is of 0.0049, and the maximum of 0.203.

The analysis of the transition points of the flow, on both sides of the foil, reveals that on the lower surface, the flow adheres practically until the trailing edge, throughout the entire angle of attack interval. On the upper surface, the flow stays laminar until 97 % of the chord at 0°, then around 2°, the separation point shifts abruptly to the leading edge, around 4 % of the chord. This value decreases with AoA increase until it can be accepted it separates on the leading edge itself.

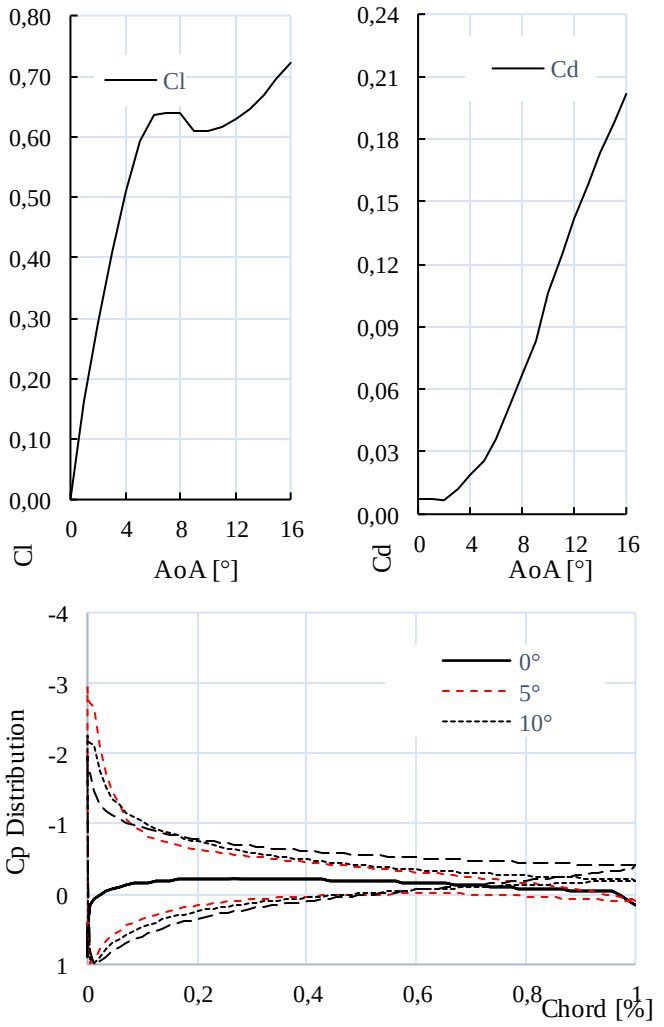

Figure 5: Plots for the C_l, C_d and C_p coefficients and transition coordinates on P113 @ Re=4.5 x10^5, XFOIL results

Aside from these results, it is important to point out that some trials were made starting at angles such as 14°, progressing to lower angles. New and different values for the coefficients were observed, adding to the previously obtained results. This is seen in figure 6, where Cl and Cd are plotted for Re 6.0x10^5.

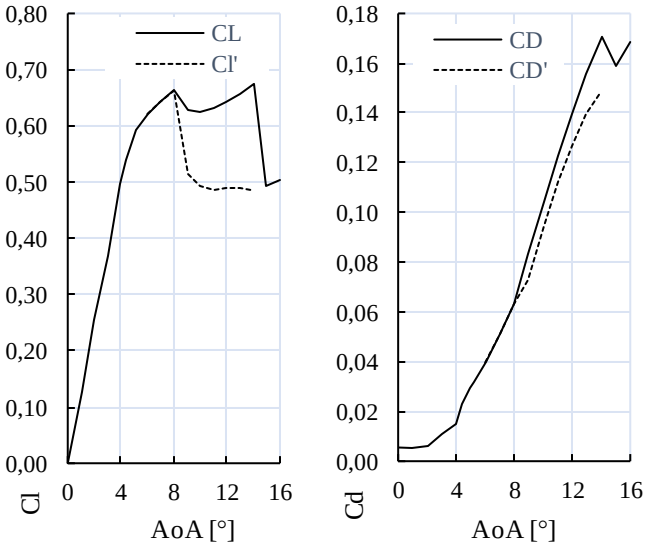

Figure 6: Plots for the C_l and C_d coefficients for P113 @ Re=6.0 x10^5, XFOIL results

This led to the conclusion that the software is finding multiple solutions for the same problem. As such, it is safe to assume that some anomaly is occurring. It would also explain the difficulty in achieving convergence on the results, as multiple solutions seem to be possible.

4 TURBULENCE AND TRANSITION MODELS VALIDATION

When concerning CDF software, one of the crucial parts is the physics' model selection. Additionally, different models need different mesh parameters. From the low Reynolds numbers used on this investigation, it is safe to assume that the laminar boundary layer is very unstable and will separate at some point along the wall. As separation occurs, the flow will have a turbulent state further downstream, with possibility of a transient state. If the turbulent flow reattaches, there may also be a separation bubble between the separation zone and reattachment. The Re and the shape of the foil influence the length of this bubble, which can be classified of short or long, the last known to be formed at Reynolds number above 5 x 10^5 [8]. This means that the separation bubble will have, eventually, different lengths along the fin.

Thus, the models should contemplate transition. For that, one turbulence model and one additional transition model, included in the software Star-CCM+ are chosen to be implemented. The first one is the *k-ω* SST turbulence model [9] and the second is the additional transition model *γ-Re$_\theta$* [10]. E387 aerofoil is used to verify the accuracy of both models comparing to wind-tunnel results.

Mesh creation was also included in the analysis. When possible, the mesh parameters are constant between the E387 and the SFWB profile and fin. The domain had to be divided into smaller volumes near the foil to refine the mesh suitably. The transition model also requires the mesh to be very fine near the surface, to capture the transition.

The simulation setup consisted of applying the next models: two-dimensional, segregated flow, liquid (at constant density), turbulent model, k – ω SST turbulence model and low Y+ wall treatment. Two simulations for each angle are performed: with transition model γ – Reθ, and without transition model (figure 7).

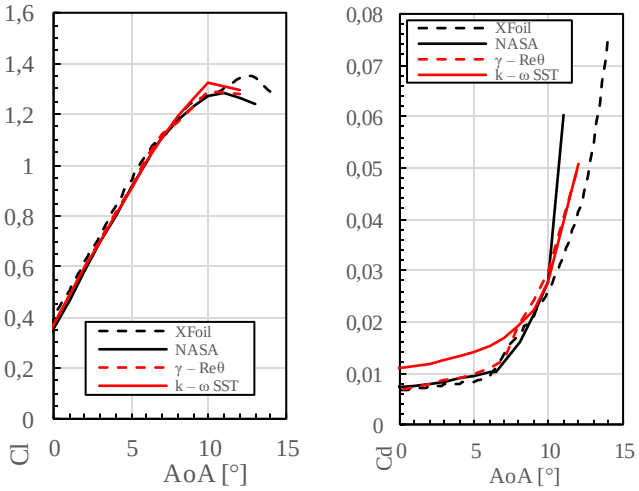

(a) Cl versus AoA, Re 4.6 x10^5 *(b) Cd versus AoA, Re 4.6 x10^5*

Figure 7: E387 lift and drag coefficients results from STAR CCM+, XFOIL and Wind-tunnel experiments

The $k-\omega$ SST performs well for lift prevision but fails for drag estimation. It is also uncapable of estimating the transition point. The reason to first consider this model was for the fact that the simulation residuals tend to converge fast, saving time, and also because there could be no transition taking place.

On the other side, adding the transition model, the lift and drag coefficients show errors of about 2% comparing to wind-tunnel tests. The transition can be estimated, although, without wind-tunnel data, it is impossible to say which of the tests performed (Star-CCM+ and XFOIL), is closer to reality.

Above 10 degrees both models present errors above 5%.

The $\gamma - Re_\theta$ will be applied to the next stages, as it is expected to estimate the lift and drag coefficients, transition and pressure closer to real experiments.

5 SWBF PROFILE PERFORMANCE

The same mesh parameters and physics' models were used as on the validation stage. For the velocity, only

three flow speeds are employed and represent the expected low, mean and top speeds the fin will experience. This way, only simulations at the Re numbers of 2.5 x10^5, 5.0 x10^5 and 7.5 x10^5 (respectively 2.100, 5.250 and 7.875 m/s), where performed. The fin chord is of 100 mm (corresponding to the length at the root).

At the beginning of simulations, especially for larger angles of attack, vortexes could be seen before the simulation converged. When the residuals drop, this instability disappears. One of the possibilities is for it to be Von Kármán vortex street, but, as simulations converge, it ceases to produce vortexes. Another option is Kelvin Helmholtz instability, which is characterised by a velocity difference, in this case, between the fluid and the fin interface. However, these instabilities do not show a great effect on the measurements. The variation of pressure and lift is approximately 10^{-3} for high AoA's. It is also confirmed that recirculation bubbles are formed. It is clear in figure 8, where a bubble forms at the leading edge and exists until 50% of the foil.

Figure 8: Q-criterion for Re 7.5 x10^5, 8° AoA

As an example, three bubbles appear in figure 9: one at the trailing edge on the pressure side, and two on the leading edge. The first one, on a), shows the flow is recirculating at the tip, but the outer layers of the flow remain laminar, as no turbulence is identified. For the leading edge, on b), the bubble seen at the pressure side is not an actual bubble but only a characteristic of the flow hitting the wall, stagnating and accelerating around it, on *-i* direction. The actual laminar separation bubble is at the suction side and, at 4 degrees, measures about 4 % of the chord length. The size of the LSB increases consistently with the progression of the AoA's and proves intrinsically connected with the stall of the profile as shown in figure 10.

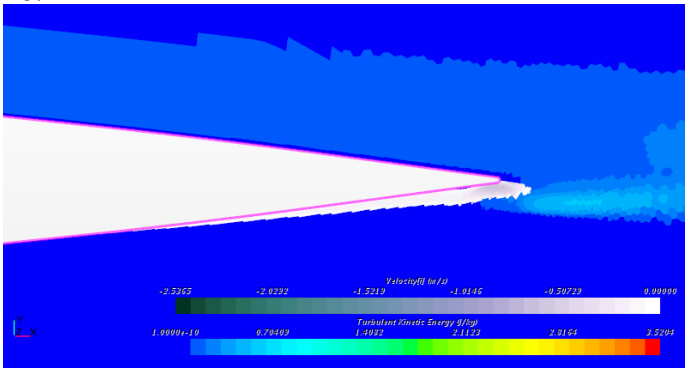

(a) Recirculation bubble at the trailing edge

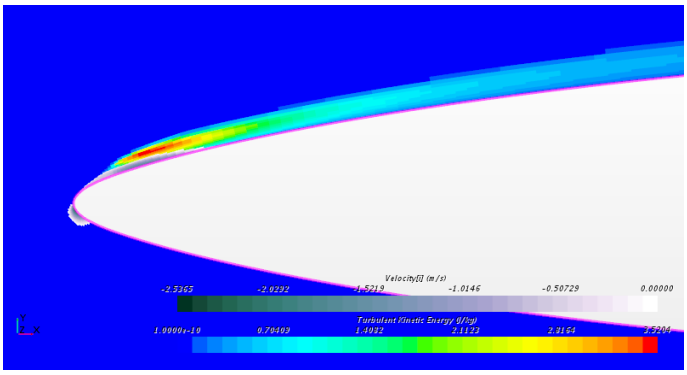

(b) Recirculation bubble at the leading edge plus stagnation point

Figure 9: Turbulent Kinetic Energy for the aerofoil P113, AoA 4°., Re: 5 x10^5, $\gamma - Re_\theta$

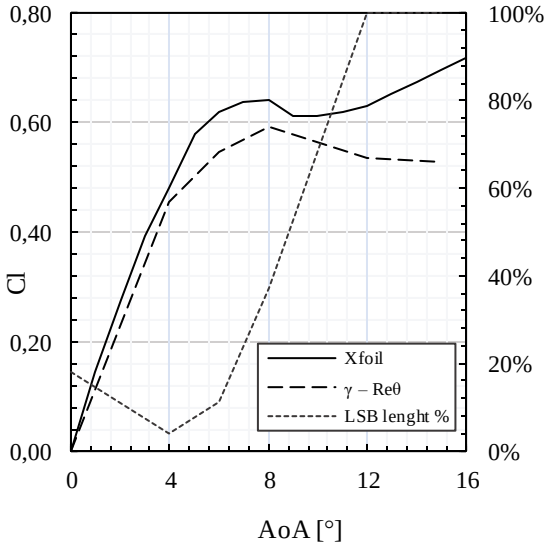

(a) C_d versus AoA and LSB length

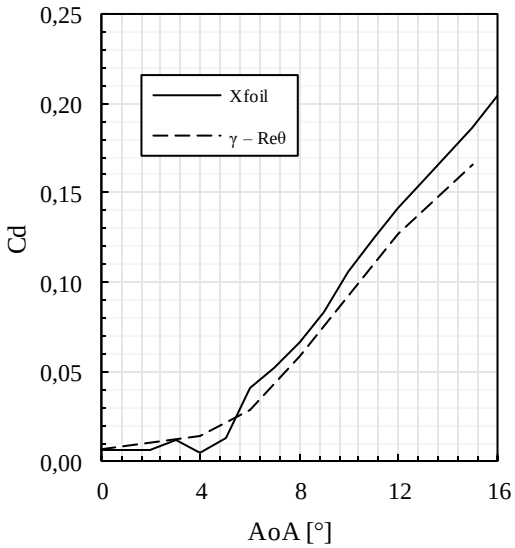

(b) C_l versus AoA

Figure 10: Lift coefficient and LSB length in chord percentage for AoA spectrum, Re: 5 x10^5, $\gamma - Re_\theta$

As seen, around 8 degrees, the size of the LSB is about 30 %. The lift coefficient drops at this point, as stall sets, this behaviour predicted at the experiments

from Lissaman P. [11]. Before, as the LSB starts to grow, the slope of the C_l starts to drop, as expected.

The values for the lift and drag coefficient, on the previous Figure 9, show how the XFOIL and Star-CCM+ may provide different results. For the lift coefficient, the obtained values are overall higher on the XFOIL simulation than the results provided on the Star-CCM+. The curve is also smoother, but that may be due to the number of samples. For the C_d, the situation is reversed: Star-CCM+ detects less drag than its counterpart. This may be due to the number of cells on Star versus the length of the panels on XFOIL. The orientation of the poor panelling distribution on XFOIL may be contributing to the increase of area in the way of the flow, making this coefficient rise.

6 SWBF OPERATION

Concerning the physics models, they are the same as used before. This way, there will be the $k - \omega$ SST turbulence model with the add-on of $\gamma - Re_\theta$. In what relates to the mesh, efforts were made to have a close mesh to the one used on the 2-D analysis, although a mesh convergence study as been made to decrease the cell number.

At the time this work was delivered, there were still simulations to be complete. For that reason, the results presented only contemplate the case at 0° for Re 5.0 x 10^5.

In what concerns the laminar separation bubble, the results from the 3-D study present a proportional LSB along three-quarters of the fin and covering 18% of the chord, and a narrower bubble near the tip (Figure 11). This bubble fades and disappears at the tip, while near the board surface it is inexistent, due to the boundary layer. It is expected that the LSB will increase chordwise on the suction side while translating towards the leading edge. These results are to be verified in future work. It will also be verified if, after 8 degrees, the bubble bursts and all the flow become turbulent.

Figure 11: LSB at the Fin, Re: 5.0 x10^5, 0° AoA

A pressure plot was obtained for the three initial sections (see figure 12). The suction and pressure symmetric sides are overlapped and, thus, only one curve for each section is depicted. Result wise; the curves illustrate the same particularities as the initial results. It is clear the small pressure increase near the leading edge, a characteristic of the fin foil. The three curves have approximately the same magnitude, indicative of a constant flow velocity spanwise.

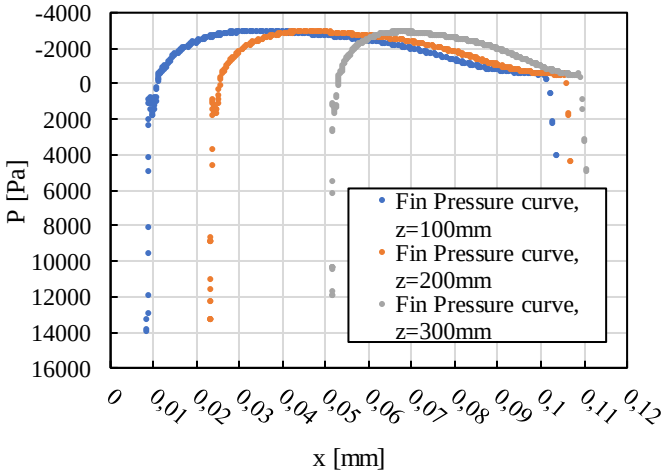

Figure 12: Fin Ox Pressure curves for AoA = 0°

Another interesting occurrence to verify is how the flow behaves after passing the recirculation bubble. After the flow recirculates, in theory, it should reattach as a turbulent boundary layer. Although this phenomenon is more noticeable for higher AoA's, it is still included in the analysis. It is expected a small band just after the LSB and at the point where in figure 12 the pressure increases, near the trailing edge. Confronting figure 13 to these suppositions proves that they do occur, as the red band symbolises the LSB and the blue band the turbulent kinetic energy, a signal for turbulent flow. It is also curious to notice the collar around the fin and the plane where the fin fits the board. At this place, the mixture between the two perpendicular flows, the one on plane xOy for the board, and the one on parallel to the surface of the fin create a zone of turbulent characteristic. Moving down in Z, it is seen that the TKE isosurface extinguishes, only to reappear at the fin tip.

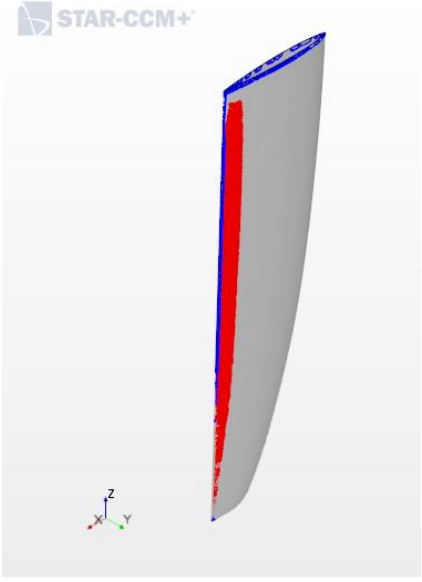

Figure 13: Turbulent Kinetic Energy (blue) and LSB (red)

In Figure 14 the high values of skin friction may be seen at the leading edge as well as a small and thin band close to the trailing edge. This band, best visible near the fin attachment to the board, is the line where the flow is reattaching as a turbulent layer. It is also seen higher friction values at the collar, at the same place where in figure 13 is found the TKE blue band.

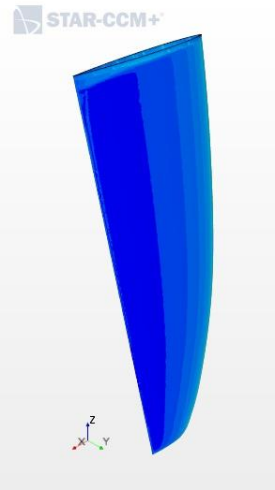

Figure 14: Skin Friction (gradient)

As part of the future work, more simulations will be done to cover the different AoA's at which the fin typically operates. It became clear that the flow is not fully laminar along the fin but has a transient behaviour. It is still to be proved that the fin generates vortexes.

7 ADDITIONAL STUDIES

7.1 *Parametric Optimisation Study*

For the first study, the XFOIL tool was once more used, making this analysis 2-D. All modifications have been achieved using the program functionalities. The modifications described are upon the actual thickness and position on maximum thickness.

The first modification concerned the maximum thickness variation. The values in chord percentage are 8.244 ±0.4122 % of chord length. The differences are minimal in the two cases. It is mainly seen that the C_l is higher in the linear region for the new cases (around 15% more), but also tends to stall before, at around a 6% lower C_l for 8 degrees. For the C_d, the +5% thickness case shows a very similar behaviour, while the decreased thickness case is showing more drag (about 10% between 5 to 9 degrees). Regarding the point of separation, almost no difference is felt on the lower side, but, for small angles of attack, the flow is separating later. For the upper side, the separation point will move to the leading edge around 2 degrees, against the 3° as on the previous analysis.

The second part is the position of maximum thickness, longitudinally along the chord, either 5% less than the original value or 5% more than it. The results look very similar to the previous ones. Most remarkably, the stall is occurring about 12% earlier (for 7 degrees). Separation is happening further on the chord, which means, the flow stays laminar for a larger foil surface.

This proves that the variation of a small percentage of thickness is enough to change the fin behaviour. This performance changes for the worse in most cases. This also shows that the fin needs to be very fine-tuned in what concerns its thickness, or the performance may be affected.

7.2 *User Profiles*

This chapter seeks to explore a visual and explicit way of telling by whom the SFWB should be used. This, together with a similar assessment for the ultimate strength, will show the stress gauge each user generates. The ultimate objective is to be able to verify the load applied to the fin and compared it to the maximum load, resulting in a user category label.

For that, three user profiles where created: a basic user, an intermediate user and a master user. For each, a probability of performing a certain manoeuvre is set (this manoeuvre is no more than speed and an angle of attack). As the names suggest, the level of expertise in each user increases, and so do the forces applied.

The idea behind it is that for each angle of attack, plus velocity, a pressure is found. The pressure results are the results obtained from previous 2-D and 3-D analysis. From it, a probability is designated to each case (velocity and AoA), and each user has a given set of cases. The sum of the probability of each case in each set generates a cumulative pressure load. It is also possible to generate the Weibull distributions for the profiles.

These results will be used later, when combined with the fatigue results, to draw a user profile performance.

7.3 *Notes on water tunnel results*

Parallel to the CFD investigation, at the Emerson Cavitation Tunnel, in Newcastle University, water tunnel tests have been conducted by Katherine Tansley.

On her research was used the same fin, like the one used on this work. The flow speed and angle of attack are changed to perform several hydrodynamic conditions. The analysis focused on the flow around the fin and the flow transition on the surface. The loads are obtained with a six-component load cell. The integral description of the assembly may be found at the disclosed work.

The main conclusions state that the fin enters in a stall at 8° of AoA and lift is the main force contributing to the resultant of forces. Additionally, it is verified that the fin tip deflects and that this deflection

rises with the flow velocity and AoA. This is an important conclusion, as the fin geometry changes, so do the behaviour of the flow. It means that the results taken by CFD analysis will lack this phenomenon, and those results will not portrait a realistic scenario. It will be vital to perform a Fluid-Structure Interaction analysis to be closer to the real-life model.

It is also interesting to verify that the deflection does not seem to decrease after the fin stalls, as one would expect after a reduction in lift.

The lift measurements are also hard to predict after 7°/8° AoA and lift is seen to be decreasing after 13.5°. The results of the lift coefficient/lift force will be posteriorly compared when more data from the CFD analysis is concluded, although the reader must bear in mind the differences in experimental and analytical results.

8 CONCLUSIONS

This work performed a hydrodynamic analysis and find how much load was at play on a slalom windsurf board fin. Since the shape of the fin's hydrofoil cannot be fit into any standard, like NACA for instance, it was mandatory to have a method to validate and calibrate the three-dynamic analysis, instead of tackling the problem directly. Thus, the task was divided into subtasks.

The first task was intended to perceive in which regime the flow is developing. This is important, as later on is explained, to select the most appropriate physical model. In this first task, the program XFOIL was used. Firstly, using a known aerofoil as a control reference (an Eppler 387), the outputs from the program were compared to real wind tunnel experiments. Knowing the abilities and limitations of the program from the simulation, the results from the fin hydrofoil were extracted. This was, most times, a hard task because the convergence of results proved difficult for AoA's between 4° and 5°. It was also needed to input a modification on the geometry of the foil. Unfortunately, XFOIL only incorporates viscosity equations, it does not solve full N-S equations. So, it cannot characterise laminar separation bubbles, and that was understood as the reason for the difficulty felt to converge certain angles.

From those notes, the second part of the three-part objective was outlined. It was clear that a transition model would have to be used, due to the flow regime and to the non-convergence of results. A 2-D-study was developed to understand which model would provide the most accurate solution. To accomplish the job, the CFD program Star-CCM+ was used. The control aerofoil was used for validation and to identify that using RANS, the SST $k - \omega$ Turbulence Model and the add-on $\gamma - Re\theta$ Transition Model would be a possible way to start the analysis.

Attention was given to the mesh characterisation. It is needed to have a good boundary layer definition to capture the transition effects. Thus, the mesh immediately around the foil needs to be constant and very fine. The method to access this is by having a Wall Y+ parameter not more than 1.

In the end, lift and pressure distributions are accurate with the chosen physics' models but should be kept in consideration that drag is represented with an error of 5%. The results with the SFWB hydrofoil revealed there was, in fact, a recirculation bubble that the XFOIL failed to represent.

There were some issues regarding 2-D solutions. From previous literature and knowledge, it was expected that the foil would shed vortexes. After intensive research, the only vortexes generated where at the first stages of the simulation, before the solution was converged. After several seconds into the simulation, there were still no signs of vortex street. This conclusion was also supported by the absence of significant pressure or force variations.

Having gathered another critical parameter, the 3-D simulation was assembled. It was designed with all the notes and results from the previous chapters. Simulations at 3-D stage progress at a smaller pace than 2-D simulations. Only one simulation case is included. The results from the first condition are unveiling results close to the two-dimensional analysis, and displaying the same flow characteristics, like the LSB.

In what concerns the parametric optimisation studies, no advantages are seen when changing the maximum thickness or its position. The path was also opened for later study of user profiles, that will need to be coordinated with a FEM analysis to the fin itself.

Finally, the parallel research in Newcastle at the cavitation tunnel shows that the fin stalls at about 8° of AoA, a number met by the present study. It also shows that the most critical force in the force resultant, measured in the SFWB, is the lift. The drag force only becomes more expressive after reaching 14°, where it increases rapidly. The fin also deflects with the hydrodynamic forces. Even after the fin stalls, the deflection does not seem to reduce, as would be expected from the lack of lift force.

The present work may be extended in the 3-D simulation. More cases are under development and when done, should provide an insight into the fin behaviour. The results will then be compared to the real-life results obtained at the cavitation tunnel.

The remaining works being developed by peers are a good add-up for the understanding of the fin. The finite element analysis that follows the hydrodynamic study in this work is already using the data provided.

It is also possible to perform a fluid-structure interaction study. This will provide results, not only for hydrodynamic and structural behaviour but also, in real time. It will become clearer why and how the fin is breaking and make a more accessible path to work on optimisation.

The hydrodynamic analysis also provided the tools and instructions for fin makers to reproduce the water effects in a non-destructive test. With this, it will be possible to achieve an enhanced fin, saving money in tests. This optimisation will give the real users improved speed and balance, as well as an overall better-quality product for less price.

Regarding competition, it will prove to be the future tool for improving this vital part of the windsurf board. Fins will be tailored for the players in less time, helping teams reach higher scores.

ACKNOWLEDGEMENTS

The author would like to thank José Chaves Pereira for the opportunity of working in LASEF, and all its team, that helped and advised on multiple occasions during the thesis. Also, to Francisco Simões for the moral support and to Luis Batista for the technical insight.

REFERENCES

[1] S. B. W. a. F. B. M. J. R. MCGhee, Experimental Results for the Eppler 387 Airfoil at Low Reynolds Numbers in the Lagley Low-Turbulence Pressure Tunnel, NASA TM-4062, October 1988.

[2] H. Y. Mark Drela, *Xfoil 6.94 User Guide*, 2001.

[3] Siemens, "STAR-CCM+ |MDX," Siemens, 2018. [Online]. Available: https://mdx.plm.automation.siemens.com/star-ccm-plus. [Acedido em 17 August 2018].

[4] M. H. Sharqawy, J. H. Lienhard e S. M. Zubair, "Thermophysical properties of seawater: A review and new correlations that include pressure dependance," *Desalination and Water Treatment*, vol. 16, pp. 354-380, April 2010.

[5] K. G. Nayar, M. H. Sharqawy, L. D. Banchik e J. H. Lienhard, "Thermophysical properties of seawater: A review and new correlations that include pressure dependance," *Desalination*, vol. 390, pp. 1-24, 2016.

[6] G. Cribb, "Tactics, Tuning and Technique," *Windsurf*, nº 298, 2010.

[7] S. M. A. Aftab, A. S. Mohd Rafie, N. A. Razak e K. A. Ahmad, "Turbulence Model Selection for Low Reynolds Number Flows," *PLos ONE*, vol. V. 11 (4), 22 April 2016.

[8] F. R. Menter, "Two-equation eddy-viscosity turbulence models for engineering applications," vol. 32, nº 8, pp. 1598-1605, 1994.

[9] F. R. Menter, R. Langtry, S. Likki, Y. Suzen, P. Huang e S. Volker, "A correlation-based transition model using local variables—Part I: model formulation," *Journal of turbomachinery*, vol. 128, nº 3, pp. 413-422, 2006.

[10] P. Lissaman, "Low-Reynolds-number airfoils," *Annual Review of Fluids Mechanics*, vol. Vol. 15, nº no. 1, pp. pp. 223-239, 1983.

[11] K. Tansley, "Investigation into Windsurf Fin Hydrodynamics - A practical Study," Newcastle University, Newcastle, 2018.